

DFT Investigation on Characteristics and Properties of Lithium Borohydride Clusters

Cheng Yang¹, Fang Li¹ and Shihai Yan^{2*}

¹College of Chemistry and Chemical Engineering, University of Jinan, Jinan, 250022, China

²College of Chemistry and Pharmaceutical Sciences, Qingdao Agricultural University, Qingdao, 266109, China

Research Article

Received date: 23/08/2017

Accepted date: 28/08/2017

Published date: 04/09/2017

*For Correspondence

Shihai Yan, College of Chemistry and Pharmaceutical Sciences, Qingdao Agricultural University, Qingdao, 266109, China. Tel: +8653286080954

E-mail: yansh@qibebt.ac.cn

Keywords: Hydrogen Storage; Density Functional Theory; Stabilization Energy; NMR Parameter

ABSTRACT

The density functional theory B3LYP method are employed to characterize the properties of the LiBH₄ clusters at the 6-311++G(d, p) basis set. The polymers from dimer to hexamer are generated through the head-to-tail coupling. The trimer may be the optimal unit for LiBH₄ clusters to combine into the natural complex. The slight variation upon electron attachment implies the strong capability of the LiBH₄ trimer (3er). The spin-spin coupling constants between Li and B can be taken as a criterion to judge the degree of polymerization and whether the additional hydride is attached or not. The theoretical hydrogen content of hydridic 3er, 3erH-, is 19.60 wt%, even higher than that of the pure LiBH₄ cluster by 1 wt %. The LiBH₄ cluster may be a good candidate to be applied in the field of hydrogen storage.

INTRODUCTION

Hydrogen, as an ideal energy carrier and pollution free, has been targeted as the utopian fuel for transportation systems. The volumetric and gravimetric density of hydrogen in the storage material is crucial for mobile applications. The hydrogen storage is one of the key challenges that must be overcome nowadays^[1-4]. The solid-state hydrogen storage material has the extraordinary superiority of providing high volumetric densities and low parasitic losses compared with those of a compressed and cryogenic hydrogen storage system. Solid-state hydrogen storage is now pursued as an effective and safe way for a routine treatment of hydrogen.

Molecular hydrogen (H₂) dissociates at the surface of hydrogen storage material upon absorption; two H atoms recombine to H₂ during the desorption process^[5]. The ideal solid hydrogen storage material for practical utilization should satisfy the following criteria: high storage capacity, reversibility, low toxicity, and low cost needed for automotive applications. The non-transition metal hydrides are generally more efficient for hydrogen storage as compared with the intermetallic hydrides owing to the involvement of lightweight elements, such as lithium, sodium, boron, and aluminum^[6-8]. Ternary boron hydrides (M_xB_yH_z, M denotes an alkali or alkaline earth), as the potential hydrogen storage materials with enhanced storage capacity (e.g., the theoretical hydrogen content of LiBH₄ and NaBH₄ is 18.36 and 10.57 wt%, respectively), have received extensive attention in recent years. The previous studies presented new insights into the metal-hydrogen bond mechanism in ternary metal hydrides and offered a possibility of synthesizing novel materials with enhanced hydrogen storage capability for practical usage^[9,10]. Although less common than NaBH₄, LiBH₄ offers some advantages, being a stronger reducing agent and highly soluble in ethers, whilst remaining safer to handle than LiAlH₄^[11]. The application of LiBH₄ is particularly advantageous in some preparations owing to its higher chemo selectivity relative to other reducing agents. LiBH₄ can also be utilized in hydrogen generation and energy storage.

Generally, the lithium borohydride is comprised of Li⁺ cation and BH₄⁻ anion, where the negative charge is allocated to the

tetrahedrally coordinated H atoms. The ionic nature of LiBH_4 offers the possibility for its clusters to host an excess electron owing to the Li^+ terminals. The additional electron may trap electron deficient H atoms and furnish a higher weight percent of hydrogen storage capacity (the targets of the U.S. Department of Energy are 6.5 wt % and 62 kg $\text{H}_2 \text{ m}^{-3}$). Thus, the excess electron system of LiBH_4 clusters may be a novel potential candidate for hydrogen storage materials. Such anions has been observed for LiAlH_4 clusters^[10]. Such anions can be generated either by injecting electrons into high-density cluster vapor^[11,12] or by attachment of low-energy electrons to preexisting clusters^[13] depending on the cluster size as extensively investigated for water clusters^[14-22]. The excess electron in a water hexamer is shared by all the participants with electropositive terminals. The similar characteristic has also been observed in anionic LiAlH_4 clusters. The dihydrogen bond has also been observed recently with experimental techniques^[23,24] and theoretical approaches^[25-27] for the existence of excess electron. The excess electron plays crucial role in the understanding of phenomena associated with electron transfers, radical chemical reactions, fission reactors, and polarons.

Here, the emphasis is put on the characteristics and properties of LiBH_4 clusters. Our investigation will shed light on the design of hydrogen storage materials and improve our understanding of excess electron. It is significant to explore characteristics such as structure, electron population, bonding, stability, and storage capacity of the LiBH_4 clusters.

COMPUTATIONAL DETAILS

Large free radicals and intermolecular complexes have been described successfully by the computationally inexpensive density functional theory^[28-30]. Especially, the hybrid B3LYP functional^[31-34] has provide its merits in dealing with valence-type molecular anions^[35-37]. Employing the B3LYP exchange-correlation functional with the 6-311++G(d, p) basis set, all calculations were performed with a suite of Gaussian 09 programs^[38]. The diffuse basis functionals were employed with a special emphasis to allow the electron spreading if the energy can be lowered and describe the expected diffusive state of the excess electron more profitably.

The zero-point vibrational energy (ZPE) was involved in the calculation for the thermodynamic stabilization energy (EO), which was obtained by subtracting the energies of monomers (neutral or negatively charged) from that of the clusters. The complexes were also characterized by using NMR parameters. The relevant NMR isotropic shielding tensors of boron and nitrogen, as well as their spin-spin coupling constants (1JB-N) were determined using the gauge-including atomic orbital method (GIAO)^[39-41] at the same level. The coupling constants include the diamagnetic spin-orbit (DSO), paramagnetic spin-orbit (PSO), Fermi-contact (FC), and the spin dipolar (SD) contributions^[42].

RESULTS AND DISCUSSION

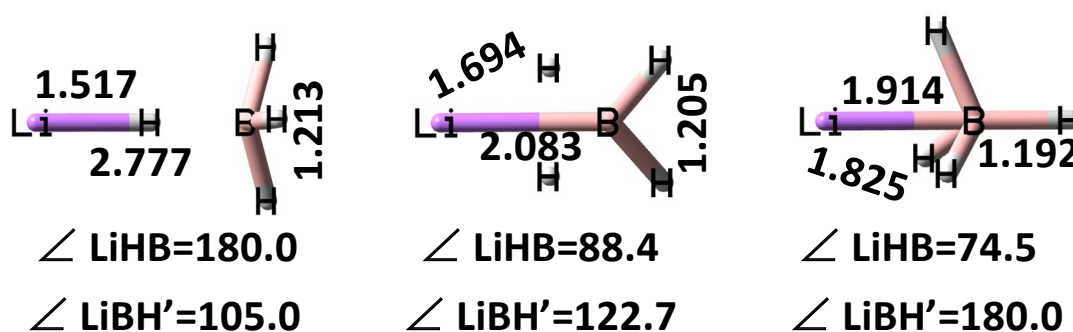


Figure 1. Optimized structures of LiBH_4 monomer and primary parameters.

Geometries

Figure 1 presents the optimized geometrical structures of the LiBH_4 monomer, where the coupling modes between the electropositive Li and the electronegative BH_4 are different. The following four phenomena are observed with the comparison of geometrical structures of the monomer. Firstly, the contact distance between Li and the hydrides extends along with the increase in number of hydrides coupled with Li. Secondly, along with the increase in number of hydrides coupled with Li, the contact distance between Li and B shortens, indicating the strengthening of Li-B interaction. Then, the bond length of B-H' (H' has no direct interaction with Li) decreases along with the same variation. At last, the angle of LiBH' increases from 105.0 to 180.0°, while the angle of LiHB decreases from 180 to 74.5° along the increase in number interacted with Li directly. The calculated geometrical parameters of tridentate isomer are in good agreement with the theoretical results obtained by Chan^[43] and Yu^[44].

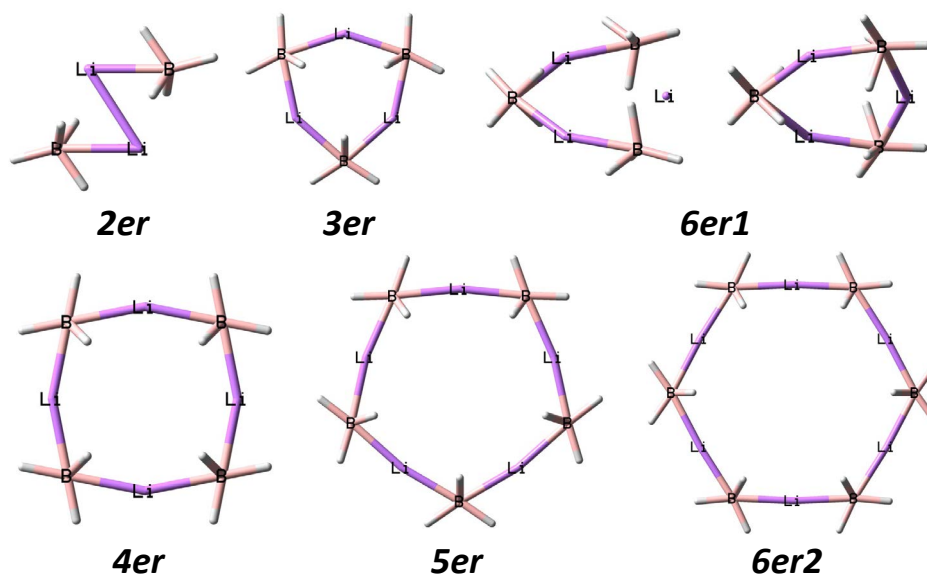


Figure 2. Optimized structures of LiBH_4 clusters from dimer (2er) to hexamer (6er).

The optimized LiBH_4 clusters from dimer to hexamer are collected in **Figure 2**. In the dimer (2er), the structure of each monomer varies owing to the interaction of Li^+ with the BH_4^- fragment of the other monomer. The Li and B atoms of 2er forms a parallelogram. The contact distance of Li-B lengthens distinctly to 2.198 Å, and the distance of Li with the other B locates at 2.276 Å. The distance of two Li^+ cations is only 2.514 Å. The BLiB and LiBLi angles are 111.6 and 68.4°, respectively. 3er is a head-to-tail-linked trimer with a D_{3h} point group. Three Li and three B atoms populates in a plane, where six hydrides locate evenly on three B atoms and point outward. The other six hydrides distribute equally on both sides of the plane determined by Li and B atoms. The distance of Li-B bond is 2.119 Å, shorter than that in 2er while longer than that in corresponding monomer.

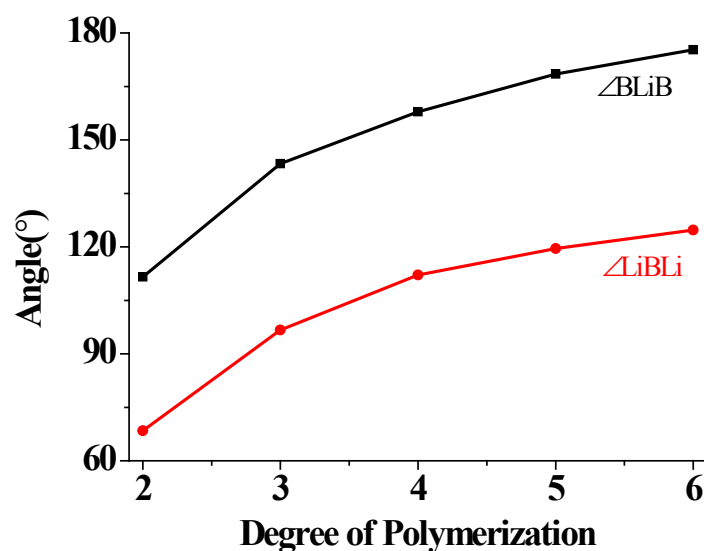


Figure 3. The BLiB and LiBLi angles in the LiBH_4 clusters.

The BLiB and LiBLi angles in 3er are 143.3 and 96.7°, respectively, larger as compared to those in 2er. A cavity is generated by three LiBH_4 monomers with a radius of 0.914 Å. The tetramer (4er) and pentamer (5er) are generated via head-to-tail polymerization, similar to that in 3er. The corresponding Li-B bond lengths in 4er and 5er are all 2.096 Å, equal to each other. The radius of the cavity in 4er and 5er is 1.739 and 2.493 Å, respectively. The BLiB and LiBLi angles in 4er and 5er increases further as compared to those in 3er, as shown in **Figure 3**. For the hexamer, two coupling modes are designed: 6er1 (two coupled rings) and 6er2 (one ring). 6er1 can be taken as the dimer of two 3er units, which are perpendicular to each other. 6er2 is composed by the head-to-tail organization with a D_{6h} point group. The Li-B bond length is 2.103 Å, slightly longer as compared to those in 4er and 5er. The electropositive Li locates between two electronegative BH_4 groups and almost in one line with two neighboring B atoms. The BLiB and LiBLi angles in 6er2 are 175.3 and 124.7°, respectively. The radius of the central cavity increases further to 3.725 Å.

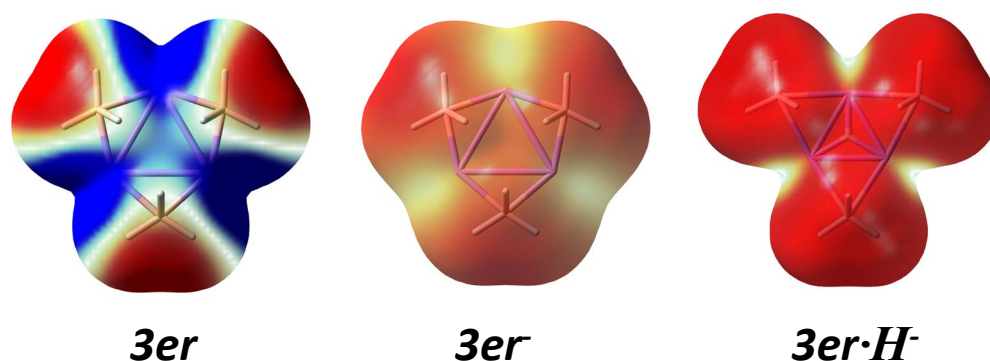


Figure 4. The electrostatic potential surfaces of trimer (3er), anionic trimer (3er⁻), and hydridic trimer (3erH⁻).

When an excess electron is injected into the cluster, the variation of the system is slight. The excess electron should locate in the middle of three Li cations, as can be drawn with the inspection of the electrostatic potential of 3er (**Figure 4**). Upon electron absorption, the changes of Li-B bond length of 2er and 3er are 0.032 and 0.011 Å, respectively. The BLiB and LiBLi angles of these two clusters alter slightly, by less than 2°. The central cavity of the 3er anion (3er⁻) (R: 0.927 Å) is a little larger than that of 3er. While the effect is significant upon absorption of an excess hydride. When the excess hydride is injected into 3er (3erH⁻), the Li-B distance extends by 0.402 Å to 2.521 Å. Three Li⁺ cations combine with the central hydride together. Thus, the distances between these cations decrease and the radius of the central cavity reduces distinctly to 0.786 Å. Simultaneously, the interaction between Li⁺ cation and BH₄⁻ anion reduces and the distance between two B atoms increases from 4.022 Å in 3er to 5.036 Å in 3erH⁻. The BLiB and LiBLi angles vary distinctly to 174.6 and 65.4°, respectively. As a comparison, the electrostatic potential surfaces of 3er⁻ and 3erH⁻ are also collected in **Figure 4**. The excess electron plays a key role to enhance the hydrogen storage capacity, as has been demonstrated previously^[10,43].

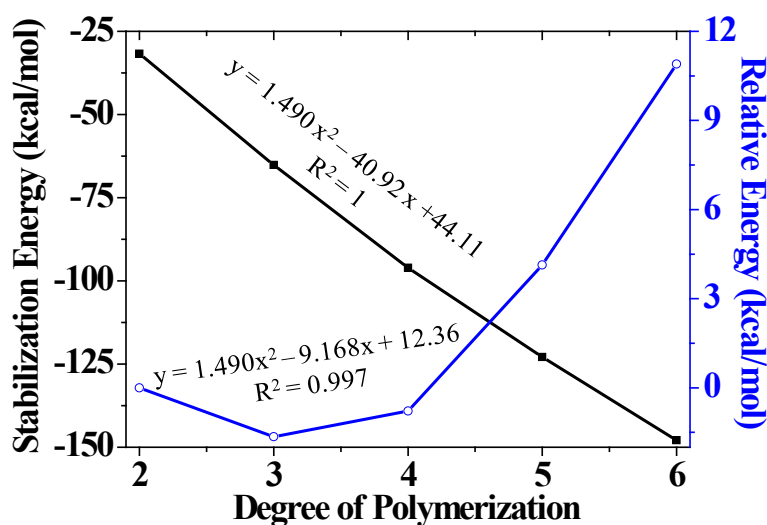


Figure 5. The stabilization energy of the polymers.

Energies

The stabilization energies (E_0) of the clusters are collected in **Figure 5**. It is obvious that the E_0 decreases along with increase of the degree of polymerization (DP) from -31.8 kcal/mol in 2er to -147.9 kcal/mol in 6er. To obtain corresponding smooth stabilization energy curves, the calculated energy points are fitted to a second order polynomial in DP. For the polynomial, the correlation coefficient, R^2 , for the fitting accuracy is equal to 1.0, indicating that the fitted curves from the calculated data are good.

As can be observed from **Figure 2** that there is only one binding site for 2er and two binding sites for 3er. Along with the increase of the cluster size, the number of the binding site augments linearly. There are 5 binding sites for 6er. To get some useful information about the optimal degree of polymerization, the variation of E_0 along with DP is fitted into a 2nd order polynomial (**Figure 5**). It is clear that the enhancement of E_0 for 3er is the largest among these clusters. Therefore, it can be proposed that the LiBH₄ monomer tends to polymerize into trimer at first, and then reorganization in 3D with this trimer as the basic unit.

The vertical electron attachment energies (E_v) of 2er and 3er are also determined at the same level. The E_v of 2er is -5.6 kcal/mol, implying that the corresponding anionic cluster is more stable as compared with 2er. While, the E_v of 3er is -1.7 kcal/mol, small as compared that of 2er. Thus, it can be drawn that the LiBH_4 cluster tends to bind an excess electron. The additional electron is helpful for further binding of excess hydrogen, therefore, the LiBH_4 cluster has the potential to be applied in the field of hydrogen storage. The hydrogen content of hydridic 3er, 3erH⁻, is 19.60 wt %, even higher than that of the pure LiBH_4 cluster by 1 wt %.

NMR Parameter

The effect of polymerization is compared with the determination of the NMR parameters (shielding tensor (σ) and spin-spin coupling constant (J)) for monomer, 3er, and 6er1. The σ of Li and B in monomer is 91.4 and 146.1 ppm, respectively. These value increase in 3er to 92.2 and 151.5 ppm, respectively. The corresponding value in 6er1 locate between those in the monomer and 3er. The coupling constant of Li and B, $^1J_{\text{Li-B}}$, in monomer, 3er, and 6er1 is 13.7, 8.6, and 4.8 Hz, respectively. The decreased value indicates the weakening of the Li-B interaction. The value of $^1J_{\text{Li-B}}$ decreases further in 3erH⁻ to 0.5 Hz, reflecting the weak interaction between Li and B. This should be the result of strong interaction between Li and the additional central hydride, the coupling constant of which, $^1J_{\text{Li-B}}$, is 25.2 Hz.

CONCLUSION

In summary, the characteristics and properties of the LiBH_4 clusters are explored employing the density functional theory B3LYP method with the 6-311++G(d, p) basis set. The polymers from dimer to hexamer are generated through the head-to-tail coupling. The trimer may be the optimal unit for LiBH_4 clusters to combine into the natural complex. The slight variation upon electron attachment implies the strong capability of the LiBH_4 trimer (3er). The spin-spin coupling constants between Li and B can be taken as a criterion to judge the degree of polymerization and whether the additional hydride is attached or not. The theoretical hydrogen content of hydridic 3er, 3erH⁻, is 19.60 wt%, even higher than that of the pure LiBH_4 cluster by 1 wt%. The LiBH_4 cluster may be a good candidate to be applied in the field of hydrogen storage.

ACKNOWLEDGMENTS

This work was supported in part by National Nature Science Foundation of China (Grant No. 21203227), Natural Science Foundation of Shandong Province (Grant No. ZR2015BM018, ZR2016BM33), and the Research Foundation for Talented Scholars of the Qingdao Agricultural University (No. 6631113335). The numerical calculations in this paper have been done on the super-computing system in the Supercomputing Center of University of Science and Technology of China.

REFERENCES

1. Lubitz W and Tumas B. Hydrogen: An Overview. *Chem Rev* 2007;107:3900.
2. Orimo S, et al. Complex Hydrides for Hydrogen Storage. *Chem Rev* 2007;107:4111.
3. Struzhkin VV, et al. Hydrogen Storage in Molecular Clathrates. *Chem Rev* 2007;107:4133.
4. Xiong ZT, et al. High-capacity hydrogen storage in lithium and sodium amidoboranes. *Nat Mater* 2008;7:138.
5. Schlapbach L and Zutte A. Hydrogen-storage materials for mobile applications. *Nature* 2001;414:353.
6. Sun Q, et al. First-Principles Study of Hydrogen Storage on $\text{Li}_{12}\text{C}_{60}$. *J Am Chem Soc* 2006;128:9741.
7. Wu H. Activation of N-Sulfonyl Oxaziridines Using Copper(II) Catalysts. *J Am Chem Soc* 2008;130:6615.
8. Balde CP. Sodium Alanate Nanoparticles. *J Am Chem Soc* 2008;130:6761.
9. Olofsson-Martensson M, et al. *J Am Chem Soc* 1999;121:10908.
10. Yan S and Lee JY. Excess Electrons in LiAlH_4 Clusters: Implication for Hydrogen Storage. *J Phys Chem C* 2009;113:1104-1108.
11. Zuttel Z, et al. LiBH_4 a new hydrogen storage material. *J Power Sources* 2003;118:1-7.
12. Haberland H, et al. Negatively charged water clusters: mass spectra of $(\text{H}_2\text{O})_n^-$ and $(\text{D}_2\text{O})_n^-$. *J Phys Chem* 1984;88:3903.
13. Knapp M, et al. Electron attachment to water clusters under collision-free conditions. *J Phys Chem* 1987;91:2601.
14. Ayotte P and Johnson MA. Water dimer to pentamer with an excess electron: Ab initio study. *J Chem Phys* 1997;106:811.
15. Silva C. Femtosecond Solvation Dynamics of the Hydrated Electron *Phys Rev Lett* 1998;80:1086.
16. Bragg AE, et al. Hydrated Electron Dynamics: From Clusters to Bulk. *Science* 2004;306:669.
17. Paik DH. Electrons in finite-sized water cavities: hydration dynamics observed in real time. *Science* 2004;306:672.
18. Hammer NI. *Science* 2004;306:675.

19. Verlet JRR, et al. *Science* 2005;307:93.
20. Turi L, et al. *Science* 2005;309:914.
21. Shkrob IA. The Structure of the Hydrated Electron. *J Phys Chem A* 2007;111:5232.
22. Zappa F, et al. Ultracold Water Cluster Anions. *J Am Chem Soc* 2008;130:5573.
23. Kevan L. Solvated electron structure in glassy matrixes. *Acc Chem Res* 1981;14:138.
24. Gutowski M, et al. *Phys Rev Lett.* 2002;88:143001.
25. Kim KS, et al. Molecular Cluster Bowl to Enclose a Single Electron. *J Am Chem Soc* 1997;119:9329.
26. Hao XY, et al. *J Chem Phys* 2003;118:83.
27. Yan S. Electron bridging dihydrogen bond in the imidazole-contained anion derivatives. *J Chem Phys* 2006;124:124314.
28. Adamo C and Barone V. In *Recent Development in Density Functional Methods*. In: Chong DP (ed.), Part II; World Scientific: Singapore, 1997.
29. Yan S and Bu Y. *J Phys Chem B* 2004;108:13874.
30. Yan S, et al. Exploration on Regulating Factors for Proton Transfer along Hydrogen-Bonded Water Chains. *Chem Phys Chem* 2007;8:944.
31. Lee C, et al. Development of the Colle-Salvetti correlation-energy formula into a functional of the electron density. *Phys Rev B* 1988;37:785.
32. Becke AD. Density-functional exchange-energy approximation with correct asymptotic behavior. *Phys Rev A* 1988;38:3098.
33. Miehlich B, et al. Results obtained with the correlation energy density functionals of Becke and Lee, Yang and Parr. *Chem Phys Lett* 1989;157:200.
34. Becke AD. Density-functional thermochemistry. III. The role of exact exchange. *J Chem Phys* 1993;98:5648.
35. Gutsev GL. Thermodynamically stability of CH₃ONO and CH₃ONO. *J Chem Phys* 1996;105:8785.
36. O'Malley PJ. The Electronic Structure of the Bacteriopheophytin a Anion Radical, in Vivo. *J Am Chem Soc* 1999;121:3185.
37. Rienstra-Kiracofe JC. Atomic and Molecular Electron Affinities. *Chem Rev* 2002;102:231.
38. Frisch MJ, et al. Gaussian 09. Revision B.01. Gaussian, Inc.: Wallingford, CT, USA; 2009.
39. Ditchfield R. Self-consistent perturbation theory of diamagnetism. *Mol Phys* 1974;27:789.
40. Dodds JL, et al. The behavior of 5H-dibenz[b,f]azepine in sulfuric acid solution. *Mol Phys* 1980;41:1419.
41. Wolinski K. Efficient implementation of the gauge-independent atomic orbital method for NMR chemical shift calculations. *J Am Chem Soc* 1990;112:8251.
42. Ramsey NF. Electron Coupled Interactions between Nuclear Spins in Molecules. *Phys Rev* 1953;91:303.
43. Chan CW and Chen HT. A computational study of LiBH₄ clusters and enhancement of their hydrogen storage by excess electrons. *Int J Energy Res* 2017;41:747-754.
44. Yu H, et al. Graphyne and Graphdiyne: Versatile Catalysts for Dehydrogenation of Light Metal Complex Hydrides. *J Phys Chem C* 2013;117:21643-21650.